Interaction of Derivatized Capped Iron(II) Porphyrin Complexes with CO and O_2

Hang Tang and David Dolphin*

Department of Chemistry, University of British Columbia, 2036 Main Mall, Vancouver, Canada V6T 1Z1

Received January 24, 1996[⊗]

A series of porphyrins strapped and capped by benzene and amidobenzene rings have been prepared. O_2 and CO bindings to their iron(II) complexes have been examined, and the role of hydrogen-bonding in stabilizing O_2 binding has been measured. Each comparison between the benzene ring (no H-bonding) and the amidobenzene ring analogues showed a free energy gain of ∼1 kcal/mol (at −45 °C) for the amidobenzene derivatives. An X-ray structure analysis was carried out for the ferric (Cl^-) complex of the benzene-capped porphyrin strapped by two butyl side chains. The crystals were monoclinic, with $a = 10.557(3)$ Å, $b = 31.290(5)$ Å, $c = 11.221(3)$ Å, $\beta = 104.62(2)°$, $Z = 4$, and space group $P2_1/n$. The structure was solved by the Patterson method and was refined by full-matrix least-squares procedures to $R = 0.040$ ($R_w = 0.041$) for 3844 reflections with $I \geq 3\sigma(F^2)$.

Introduction

The protein environments surrounding the heme moiety play key roles in dioxygen and carbon monoxide binding to hemeproteins. Hemoglobin has a lower affinity for carbon monoxide relative to dioxygen[1,2] when compared with simple iron−porphyrin systems, due to the steric hindrance on the distal side of the heme,[2,3−6] porphyrin skeletal deformations,[7,8] and polar factors associated with the distal pocket. However, the predominant hypothesis as to how heme proteins suppress CO binding was recently challenged.[9] Stabilization of bound dioxygen through hydrogen-bonding with the His E7 residue of hemoglobin was first suggested as a consequence of the end-on coordinated geometry in the distal pocket predicted by Pauling.[10] Infrared,[11] resonance Raman,[12] kinetic,[13] and ESR studies[14] of some myoglobins and hemoglobins have all provided evidence for such hydrogen-bonding. Direct evidence of H-bonding was provided by a neutron diffraction study of oxymyoglobin that yielded an N−H···O_2 distance of 2.97 Å.[15] This was followed by an X-ray analysis[16] of oxyhemoglobin which gave N−H···O_2 distances of 2.7 and 3.2−3.4 Å for the α and β subunits, respectively, suggesting stronger H-bonding in the α subunit than in the β subunit.

In response to the complexity imposed by the protein pocket around the heme, a great deal of work has been devoted to the development of model systems where the influence of the immediate protein environment on ligand binding can be evaluated separately by designing different model compounds. Many iron(II) porphyrin (heme) models which are capable of reversibly binding carbon monoxide and dioxygen have been synthesized and studied.[17−24] Nature has designed hemoglobin and myoglobin for their ability not only to reversibly bind dioxygen but to specifically discriminate against CO binding, a critical requirement since mammals produce sufficient CO, from the natural degradation of heme,[25] to saturate any simple ferrous porphyrin not designed to raise $K_{1/2}^{CO}$. It is especially interesting to note that Collman and his colleagues[24] recently made a capped porphyrin which is unique in that it does not bind CO even at 1 atm but reversibly binds dioxygen at room temperature in the presence of nitrogenous axial bases.

[⊗] Abstract published in *Advance ACS Abstracts,* June 15, 1996.

(1) Collman, J. P.; Brauman, J. I.; Halbert, T. R.; Suslick, K. S. *Proc. Natl. Acad. Sci. U.S.A.* **1976**, *73*, 3333−3337.
(2) Heidner, E. J.; Ladner, R. C.; Perutz, M. F. *J. Mol. Biol.* **1976**, *104*, 707−722.
(3) Baldwin, J. M. *J. Mol. Biol.* **1980**, *136*, 103−128.
(4) Kuigan, J.; Wilz, S.; Karplus, M.; Petsko, G. A. *J. Mol. Biol.* **1986**, *192*, 133−154.
(5) Norvell, J. C.; Nunes, A. C.; Schoenborn, B. P. *Science* **1975**, *192*, 568−570.
(6) Peng, S.-M.; Ibers, J. A. *J. Am. Chem. Soc.* **1976**, *98*, 8032−8036.
(7) Derewenda, Z.; Dodson, G ; Emsley, P.; Harris, D.; Nagai, K.; Perutz, M. F.; Renaud, J.-P. *J. Mol. Biol.* **1990**, *211*, 515−519.
(8) Kim, K.; Fettinger, J.; Sessler, J. L.; Cyr, M.; Hugadahl, J.; Collman, J. P.; Ibers, J. A. *J. Am. Chem. Soc.* **1989**, *111*, 403−405.
(9) Lim, M.; Jackson, T. A.; Anfinrud, P. A. Science, **1995**, *269*, 962−966.
(10) Pauling, L. *Nature*, **1964**, *203*, 182−183.
(11) (a) Barlow, C. H.; Maxwell, J. C.; Wallace, W. J.; Caughey, W. S. *Biochem. Biophys. Res. Commun.* **1973**, *55*, 91−95. (b) Maxwell, J. C.; Volpe, J. A.; Barlow, C. H.; Caughey, W. S. *Biochem. Biophys. Res. Commun.* **1974**, *58*, 166−171.
(12) Tsubaki, M.; Yu, N.-T. *Proc. Natl. Acad. Sci. U.S.A.* **1981**, *78*, 3581−3585.
(13) Mims, M. P.; Porras, A. G ; Olson, J. S.; Noble, R. W.; Peterson, J. A. *J. Biol. Chem.* **1983**, *258*, 14219−14232.
(14) (a) Yonetani, T.; Yamamoto, H.; Iizuka, T. *J. Biol. Chem.* **1974**, *249*, 2168−2174. (b) Walker, F. A.; Bowen, J. *J. Am. Chem. Soc.* **1985**, *107*, 7632−7635. (c) Ikeda-Saito, M.; Iizuka, T.; Yamamoto, H.; Kayne, F. J.; Yonetani, T. *J. Biol. Chem.* **1977**, *252*, 4882−4887.
(15) Phillips, S. E. V.; Schoenborn, B. P. *Nature* **1981**, *292*, 81−82.
(16) (a) Shaanan, B. *J. Mol. Biol.* **1983**, *171*, 31−59. (b) Shaanan, B. *Nature* **1982**, *296*, 683−684.
(17) Momenteau, M.; Reed, C. A. *Chem. Rev.* **1994**, *94*, 659−698.
(18) (a) Traylor, T. G.; Tsuchiya, G.; Campbell, D.; Mitchell, M.; Stynes, D.; Koga, N. *J. Am. Chem. Soc.* **1985**, *107*, 604−614. (b) Traylor, T. G.; Koga, N.; Deardurff, L. A.; Swepston, P. N.; Ibers, J. A. *J. Am. Chem. Soc.* **1984**, *106*, 5132−5143. (c) Traylor, T. G.; Koga, N.; Deardurff, L. A. *J. Am. Chem. Soc.* **1985**, *107*, 6504−6510.
(19) Collman, J. P.; Brauman, J. I.; Iverson, B. L.; Sessler, J. L.; Morris, R. M.; Gibson, Q. H. *J. Am. Chem. Soc.* **1983**, *105*, 3052−3064.
(20) (a) Hishimoto, T.; Dyer, R. L.; Crossley, M. J.; Baldwin, J. E.; Basolo, F. *J. Am. Chem. Soc.* **1982**, *104*, 2101−2109. (b) Rose, J. E.; Venkatasubramanian, P. N.; Swartz, J. C.; Jones, R. D.; Basolo, F.; Hoffman, B. M. *Proc. Natl. Acad. Sci. U.S.A.* **1982**, *79*, 5742−5745.
(21) Suslick, K. S.; Fox, M. M.; Reinert, T. J. *J. Am. Chem. Soc.* **1984**, *106*, 4522−4525.
(22) (a) Ward, B.; Wang, C.; Chang, C. K. *J. Am. Chem. Soc.* **1981**, *103*, 5236−5238. (b) Chang, C. K.; Ward, B.; Young, R.; Kondylis, M. *J. Macromol. Sci., Chem.* **1988**, *A25*, 1307−1326. (c) Chang, C. K.; Kondylis, M. P. *J. Chem. Soc., Chem. Commun.* **1986**, 316−318.
(23) (a) Momenteau, M.; Lavalette, D. *J. Chem. Soc., Chem. Commun.* **1982**, 341−343. (b) Momenteau, M.; Loock, B.; Lavalette, D.; Tetreau, C.; Mispelter, J. *J. Chem. Soc., Chem. Commun.* **1983**, 962−964.
(24) Collman, J. P.; Zhang, X.; Hermann, P. C.; Uffelman, E. S.; Boitrel, B.; Straumanis, A.; Brauman, J. I. *J. Am. Chem. Soc.* **1994**, *116*, 2681−2682.
(25) Schmid, R.; McDonagh, A. F. In *The Porphyrins*; Dolphin, D., Ed.; Academic Press: New York, 1978; Vol. VI, pp 257−292.

S0020-1669(96)00074-2 CCC: $12.00

Establishment of ligand-binding properties by heme proteins has been largely attributed to model studies. Some of the model systems have been selectively designed to probe the polar effect within the distal heme pocket,[18,21,22,26] and their thermodynamic and kinetic data have provided quantitative evidence for H-bonding between O_2 and His E7. The roles of distal hydrogen-bonding and synthetic heme dioxygen complexes were recently thoroughly reviewed.[17]

Research in this field from our department has led to the development of durene-capped heme systems (**1a**−**c**)[27] with

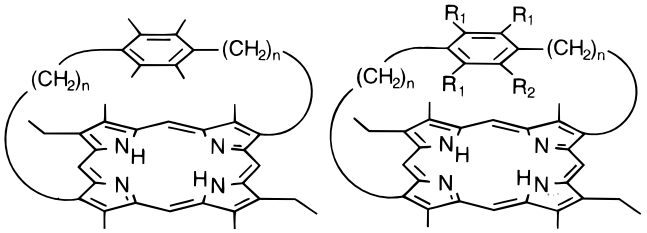

1a: n = 4
1b: n = 5
1c: n = 7

2a: n = 4
2b: n = 5
} $R_1 = R_2 = H$
2c: n = 4
2d: n = 5
} $R_1 = H$, $R_2 = NHCOCH_3$

fully hydrophobic cavities. The influence of distal side hindrance and porphyrin skeletal doming on ligand binding has been examined in the absence of stabilizing polar interactions.[28] However, lack of polar factors on the distal side in these systems has led generally to poor differentiation between CO and O_2.[28d] In order to address this problem, amide-substituted-benzene-capped and unsubstituted-benzene-capped porphyrin model systems (**2a**−**d**)[29] have been designed and synthesized to clarify the contribution of electrostatic effects to the discriminatory binding of CO and O_2 by hemoglobin and myoglobin. We present here the results of O_2- and CO-binding studies carried out on these new model systems.

Experimental Section

Preparations and General Procedures. Toluene was washed with concentrated H_2SO_4 and H_2O and distilled over CaH_2. 1,5-Dicyclohexylimidazole (DcIm, Aldrich) was recrystallized from heptane. CO and O_2 were passed through a KOH column prior to use. N_2 was initially passed through a Ridox column and then dried over molecular sieves and KOH to remove any trace O_2 and H_2O. The solubilities of CO and O_2 in toluene were taken as 1.0×10^{-5} and 1.2×10^{-5} M/Torr, respectively, at 20 °C.[30]

The preparation of the free-base benzene-capped and amidobenzene-capped porphyrins has been described previously.[29]

The hemin chlorides [Fe^{III}(Por)Cl, Por = dianion of the derivatized capped porphyrins] were prepared by adding the free-base porphyrin (0.035 mmol) in THF (20 mL) to a stirred solution of ferrous chloride (0.35 mmol) in MeOH (20 mL) under N_2 and refluxing for 1.5 h. The solution was cooled and stirred in air for 30 min. The solvent was then evaporated *in vacuo*, and the residue was washed with CH_2Cl_2/H_2O and chromatographed on alumina (30 g, 4% H_2O added) using CH_2Cl_2 as the eluent. The green μ-oxo dimer, eluting from the column, was shaken with aqueous HCl (0.2 M, 30 mL) and the resulting hemin chloride crystallized from MeOH/CH_2Cl_2; yield ∼80%.

2a$^+$Cl$^-$ mol wt: calcd for $FeC_{42}H_{46}N_4Cl$, 697.2760; found by high-resolution mass spectrometry, 697.2756

visible data (toluene)

λ_{max} (nm)	374	402 (sh)	508	528	630
log ϵ	4.74	4.67	3.80	3.82	3.56

2b$^+$Cl$^-$ mol wt: calcd for $FeC_{44}H_{50}N_4Cl$, 725.3073; found by high-resolution mass spectrometry, 725.3098

visible data (toluene)

λ_{max} (nm)	380	400 (sh)	508	532	632
log ϵ	4.86	4.77	3.73	3.77	3.33

2c$^+$Cl$^-$ mol wt: calcd for $FeC_{44}H_{49}N_5OCl$, 754.2975; found by high-resolution mass spectrometry, 754.2977

visible data (toluene)

λ_{max} (nm)	380	402 (sh)	494	534	630
log ϵ	4.78	4.70	3.98	3.85	3.60

2d$^+$Cl$^-$ mol wt: calcd for $FeC_{46}H_{53}N_5OCl$, 782.3288; found by high-resolution mass spectrometry, 782.3267

visible data (toluene)

λ_{max} (nm)	380	400 (sh)	508	532	632
log ϵ	4.88	4.79	3.78	3.82	3.43

Elemental analyses were obtained for the free bases,[29] but the iron complexes could not be satisfactorily combusted.

Reduction of hemin (Fe^{III}) chlorides was achieved by following the procedure described previously.[28b] Five-coordinate iron(II) complexes Fe(Por)(DcIm) [Fe(Por)B] were prepared in toluene via reduction of the hemin chloride using aqueous sodium dithionite, in the presence of DcIm of an appropriate concentration. After being dried (Na_2SO_4 followed by CaH_2), the Fe^{II}(Por)(DcIm) solution was transferred directly into a specially designed tonometer. CO or O_2 mixtures, prediluted with nitrogen, were admitted using a manometer, and the heme solution was allowed to equilibrate to the desired temperature. For low temperatures (−45 °C), a 6 cm length quartz cell mounted inside a small Dewar flask filled with a chlorobenzene−liquid nitrogen slush was used. Spectra were recorded on a Hewlett Packard 8452A diode array spectrophotometer in the range 250−700 nm.

For infrared measurements, carbon monoxide at 1 atm was admitted into the concentrated 5-coordinated heme solutions, prepared according to the above method, to generate Fe(Por)(DcIm)(CO) complexes. Concentrations were [heme] ∼ 0.01 M and [DcIm] ∼ 1 M, ensuring that base displacement by CO did not occur on the unhindered side of the heme. About 0.25 mL of the solution was withdrawn using a gastight micrometer syringe and placed into an IR solution cell (KBr windows) purged with CO. Carbonyl stretching frequencies of Fe^{II}(Por)(DcIm)(CO) complexes were recorded on an ATI Mattson Genesis Series Fourier transform IR spectrometer. An IR spectrum of a toluene solution, containing DcIm at ∼1 M and saturated with 1 atm CO, was subtracted from that of each Fe(Por)(DcIm)(CO) complex to obtain ν(CO).

X-ray Crystallographic Analysis of the Ferric (Cl$^-$) Complex of 2a. Crystallographic data are given in Table 1. The final unit cell parameters were obtained, using a dark green crystal (0.2 × 0.25 × 0.43 mm prism) grown from methanol, by least-squares calculations on the setting angles for 25 reflections with $2\theta = 25.1-33.8°$. The intensities of three standard reflections, measured every 200 reflections throughout the data collection, showed only small random variations. The data were processed[31] and corrected for Lorentz and polarization effects and for absorption (empirical; based on azimuthal scans for three reflections).

The structure was solved by conventional heavy-atom methods, the coordinates of the Fe and Cl atoms being determined from the Patterson

(26) Collman, J. P.; Zhang, X.; Wong, K.; Brauman, J. I. *J. Am. Chem. Soc.* **1994**, *116*, 6245−6251.
(27) (a) David, S.; Dolphin, D.; James, B. R.; Paine, J. B., III; Wijesekera, T. P.; Einstein, F. W. B.; Jones, T. *Can. J. Chem.* **1986**, *64*, 208−212. (b) Wijesekera, T. P.; David, S.; Paine, J. B., III; James, B. R.; Dolphin, D. *Can. J. Chem.* **1988**, *66*, 2063−2071.
(28) (a) David, S.; Dolphin, D.; James, B. R. In *Frontiers of Bioinorganic Chemistry*; Xavier, A. V., Ed.; VCH Verlagsgesellschaft: Weinheim, Germany, 1985; p 163−182. (b) David, S.; James, B. R.; Dolphin, D. *J. Inorg. Biochem.* **1986**, *28*, 125−135. (c) David, S.; James, B. R.; Dolphin, D. *Can. J. Chem.* **1987**, *65*, 1098−1102. (d) David, S.; James, B. R.; Dolphin, D.; Traylor, T. G.; Lopez, M. *J. Am. Chem. Soc.* **1994**, *116*, 6−14.
(29) (a) Tang, H.; Wijesekera, T. P.; Dolphin, D. *Can. J. Chem.* **1992**, *70*, 1366−1374. (b) Tang, H. Ph.D. Dissertation, University of British Columbia, 1990.
(30) Linke, W. R.; Seidell, A. *Solubilities of Inorganic and Metal-Organic Compounds*; Van Nostrand: Princeton, NJ, 1958.
(31) *TEXSAN Crystal Structure Analysis Package*, Version 5.1; Molecular Structure Corp.: The Woodlands, TX, 1985.

Table 1. Crystallographic Data for the Ferric (Cl^-) Complex of **2a**[a]

formula	$C_{42}H_{46}ClFeN_4$
fw	698.15
crystal system	monoclinic
space group	$P2_1/n$
a, Å	10.557(3)
b, Å	31.290(5)
c, Å	11.221(3)
β, deg	104.62(2)
V, Å^3	3587(3)
Z	4
ρ_{calcd}, g/cm^3	1.293
ρ_{obsd}, g/cm^3	not measured
$F(000)$	1476
radiation (λ, Å)	Mo (0.710 69)
T, °C	21
μ, cm^{-1}	5.28
crystal size, mm	0.20 × 0.25 × 0.43
transm factors (rel)	0.94−1.00
scan type	ω
scan range, deg in ω	1.32 + 0.35 tan θ
scan speed, deg/min	32 (up to 8 rescans)
data collected	$+h,+k,\pm l$
$2\theta_{max}$, deg	55
crystal decay, %	negligible
no. of tot. reflns	8854
no. of unique reflns	8416
R_{merge}	0.035
no. of reflns with $I \geq 3\sigma(F^2)$	3844
no. of variables	433
R	0.040
R_w	0.041
gof	1.77
max Δ/σ (final cycle)	0.03
residual density, e/Å^3	−0.32 to +0.24

[a] Temperature 294 K, Rigaku AFC6S diffractometer, graphite monochromator, takeoff angle 6.0°, aperture 6.0 × 6.0 mm at a distance of 285 mm from the crystal, stationary background counts at each end of the scan (scan/background time ratio 2:1), $\sigma^2(F^2) = [S^2(C + 4B) + 0.02F_o^2)^2]/(L_p)^2$ (S = scan rate, C = scan count, B = normalized background count), function minimized $\sum w(|F_o| - |F_c|)^2$ where $w = 4F_o^2/\sigma^2(F_o^2)$, $R = \sum||F_o| - |F_c||/\sum|F_o|$, $R_w = (\sum w(|F_o| - |f_c|)^2/\sum w|F_o|^2)^{1/2}$, and gof $= [\sum w(|F_o| - |F_c|)^2/(m - n)]^{1/2}$. Values given for R, R_w, and gof are based on those reflections with $I \geq 3\sigma(F^2)$.

function and those of the remaining atoms from subsequent difference Fourier syntheses. The non-hydrogen atoms were refined with anisotropic thermal parameters. Hydrogen atoms were visible on difference maps and were included in idealized positions (C−H = 0.98 Å, B(H) = 1.2B(parent atom)). The hydrogen atoms of two methyl groups (C(35) and C(40)) were modeled as 1:1 disordered. Neutral-atom scattering factors and anomalous-dispersion corrections were taken from ref 32.

Selected bond lengths and angles are given in Table 2. Atomic coordinates, anisotropic thermal parameters, bond lengths, bond angles, torsion angles, intermolecular contacts, and least-squares planes are included as Supporting Information. Structure factors are available from the authors upon request.

Results and Discussion

To prevent small imidazoles from binding under the cap of the heme, leading to the formation of 6-coordinate hemochromes, the sterically hindered base 1,5-dicyclohexylimidazole (DcIm, **B**) was chosen for the CO- and O_2-binding studies with the present systems, on the basis of earlier studies of the durene[28b] and other systems.[18a,20a] After reduction of the ferric complexes, visible spectral changes indicated a typical 5-coordinate species had been formed. During the titration, a large excess of DcIm (0.1−0.3 M) was maintained in solution to ensure that the observed changes corresponded exclusively to the binding of CO and O_2 on the capped side of the heme.

Table 2. Selected Bond Lengths (Å) and Bond Angles (deg) for the Ferric (Cl^-) Complex of **2a**

Fe(1)−Cl(1)[a]	2.225(1)	Fe(1)−N(3)	2.059(3)
Fe(1)−N(1)	2.061(1)	Fe(1)−N(4)	2.055(3)
Fe(1)−N(2)	2.063(1)		
Cl(1)−Fe(1)−N(1)	107.44(8)	N(1)−Fe(1)−N(3)	147.1(1)
Cl(1)−Fe(1)−N(2)	105.33(8)	N(1)−Fe(1)−N(4)	87.0(1)
Cl(1)−Fe(1)−N(3)	105.47(8)	N(2)−Fe(1)−N(3)	87.3(1)
Cl(1)−Fe(1)−N(4)	100.05(9)	N(2)−Fe(1)−N(4)	154.6(1)
N(1)−Fe(1)−N(2)	85.6(1)	N(3)−Fe(1)−N(4)	85.9(1)

[a] See Figure 4 for numbering system.

CO Binding. The 5/5-heme (**2b**) was found to bind CO too strongly to allow K_B^{CO} to be determined using pure CO, and even for the 4/4-heme (**2a**), $P_B^{CO_{1/2}}$ was only a few Torr and accurate addition of pure CO during titration was difficult. Therefore, CO/N_2 mixtures were used. Qualitative studies of the open face binding of CO gives a Soret band at 394 nm, whereas CO binding under the cap results in a Soret band at 416 nm. Thus the equilibrium constant K_B^{CO} obtained for each heme (Soret at 416 nm for the carbonyl) corresponds exclusively to the binding of CO on the capped side of the heme, without any complication caused by displacement of the DcIm axial base.

The spectral properties of the 4-, 5-, and 6-coordinate **2a** complexes are shown in Figure 1. All of the K_B^{CO} values were obtained via addition of CO/N_2 mixtures to the 5-coordinate hemes, according to eq 1.

$$\text{Fe(Por)(DcIm)} + \overset{K_B^{CO}}{\rightleftharpoons} \text{Fe(Por)(DcIm)(CO)} \qquad (1)$$

In all cases, the data were analyzed according to the standard Hill equation.[33] An example of the isosbestic spectral changes and isosbestic points observed for CO binding is shown in Figure 2 and the corresponding Hill plot in Figure 3. The K_B^{CO} values together with those for the unsubstituted durene series and open chelated systems are shown in Table 3.

The results show that there has been a remarkable reduction in CO affinities with our system compared to the corresponding durene series (**1a**−**c**) and the "open" chelated proto- (**3a**) and mesoheme (**3b**) systems. The 5/5-capped complex (**2b**) exhibited a 100-fold reduction in CO affinity and the 4/4-capped complex (**2a**) a 10^4-fold reduction compared to those of the "open" chelated hemes. The complexes reported here discriminate against CO binding so strongly that the 5-coordinate species could be readily regenerated by pumping. Normally, pumping CO complexes such as chelated protoheme[34] would not remove

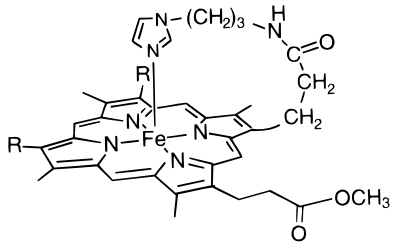

3a: R = vinyl
3b: R = Et

(32) *International Tables for X-Ray Crystallography*; Kynoch Press: Birmingham, England, 1974; Vol. IV, pp 99−102 and 149.
(33) (a) Hill, A. V. *J. Physiol. (London)* **1910**, *40*, IV−VII. (b) Ellis, P. E.; Linard, J. E.; Szymanski, T.; Jones, R. D.; Budge, J. R.; Basolo, F. *J. Am. Chem. Soc.* **1980**, *102*, 1889−1896.
(34) Traylor, T. G.; Mitchell, M. J.; Tsuchiya, S.; Campbell, D. H.; Stynes, D. V.; Koga, N. *J. Am. Chem. Soc.* **1981**, *103*, 5234−5236.

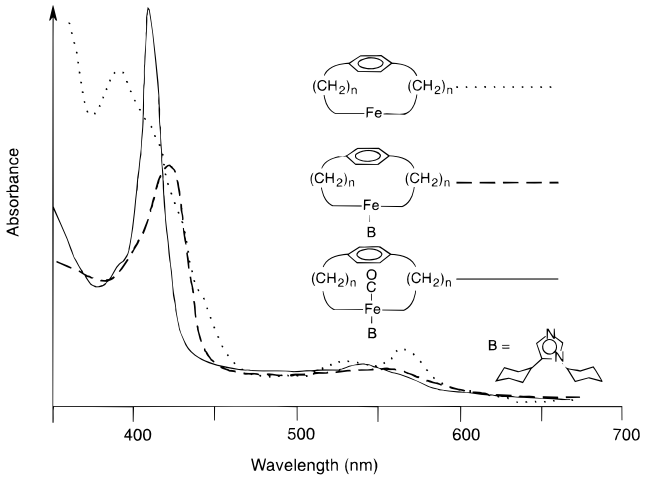

Figure 1. Spectral trends for the 4-, 5-, and 6-coordinate ferrous complexes of **2a** ($n = 4$).

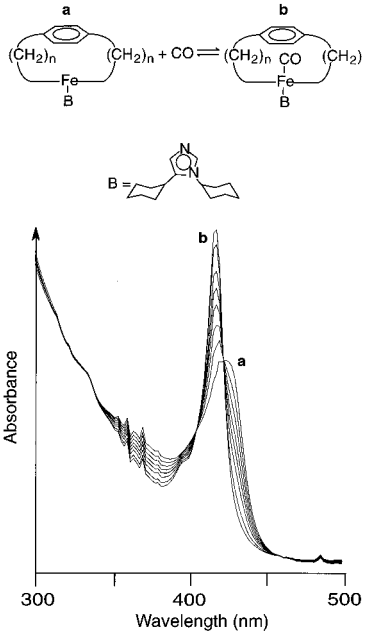

Figure 2. Isosbestic changes observed during the carbonylation of **2a** ($n = 4$) at −20 °C in toluene. $P^{CO} = 1.99$, 4.30, 7.55, 11.60, 19.03, 34.64, 51.87 Torr. Final $P^{CO} = 1$ atm.

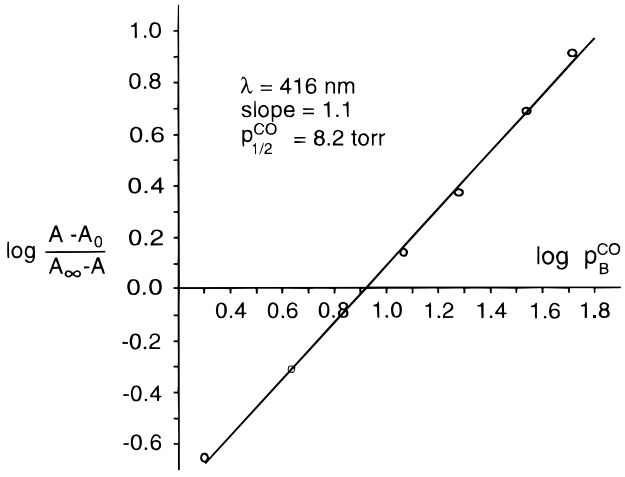

Figure 3. Hill plot for CO binding to **2a**.

the bound CO. Compared to the case of the durene series, the reduction in CO affinities is still large, with 50- and 350-fold decreases for **2b** and **2a**, respectively. At first, the results seemed unexpected because the caps of the durene system should be more crowded and access to the central metal should be even more hindered. However, placement of a more rigid diagonal strap (i.e. the durene moiety) relative to the benzeneand amidobenzene analogues induces doming of the porphyrin skeleton and results in a greater accessibility for an incoming ligand to Fe(II), thus effectively enhancing K_B^{CO}.[28d] On the other hand, the more flexible benzene and amidobenzene moieties might be suspended closer to the center of the porphyrin plane and to the iron. This is manifested in the crystal structure for the ferric (Cl^-) complex of **2a** (Figure 4). A 100-fold lower CO affinity for **2a** compared to **2b** was observed and presumably results from the increased distortion of the porphyrin skeleton and a more crowded distal side of the heme. The shortened strap over the distal side of **2a** should result in a more distorted porphyrin with more "T-state" character and a lower CO affinity. The similar K_B^{CO} values of Fe(benzene-Por)(DcIm) and Fe(amidobenzene-Por)(DcIm) are consistent with the anticipated lack of a polar effect on CO binding due to the near electrical neutrality of an Fe−C−O unit.

Table 3. Equilibrium Constants for Co Binding to Hemes in Toluene

heme	no.	K_B^{CO}, M^{-1}	$10^4 P_{1/2}^{CO}$, Torr
durene-4/4 (B)[a]	**1a**	4.3×10^6	15.0
durene-5/5 (B)[a]	**1b**	8.6×10^7	11.2
durene-7/7 (B)[a]	**1c**	6.6×10^7	230
benzene-4/4 (B)	**2a**	1.2×10^4	82000
benzene-5/5 (B)	**2b**	1.6×10^6	610
amidobenzene-4/4 (B)	**2c**	2.8×10^4	36000
amidobenzene-5/5 (B)	**2d**	3.3×10^6	300
chelated protoheme[b]	**3a**	4.0×10^8	2.5
chelated mesoheme[b]	**3b**	2.0×10^8	5.0

[a] Reference 28d. [b] Reference 34; solvent toluene−CH_2Cl_2 (9:1).

For the Fe(benzene-4/4)(DcIm) and Fe(amidobenzene-4/4)(DcIm) systems, K_B^{CO} values were measured at different temperatures within the range 0−30 °C. The thermodynamic constants $\Delta H°_{CO}$ and $\Delta S°_{CO}$ were obtained by Van't Hoff plots of ln K_B^{CO} vs $1/T$ (K), shown in Figures 5 and 6. Table 4 gives the thermodynamic data for CO binding of the benzene- and amidobenzene-4/4 hemes together with data for the durene series. It is clear that the relative decrease in CO affinity in our system results from the more unfavorable entropy change. The large entropy loss suggests more rigidity of the CO complexes of the 4/4-benzene and amidobenzene hemes relative to those of the durene systems. After formation of the CO complex, perhaps the previously flexible benzene moiety becomes less mobile and the low CO affinities could be rationalized by the relatively large overall loss of translational entropy (more negative $\Delta S°$) of the reacting porphyrin species.

We have measured ν(CO) values for compounds **2a**−**d** (Table 5) and find that they are similar to those measured for **1a**,**b**. Even though these values are among some of the highest recorded for carbonyls in model heme systems, it is difficult to interpret the data when one remembers that a change of 10 cm^{-1} represents a change of less than 0.03 kcal mol^{-1}. Moreover, it is clear that interpretations of CO stretching frequencies cannot be reduced to too simplistic a level[18a] and that only very detailed studies can hope to begin to correlate infrared frequencies to geometric, steric, or electronic interactions and polar effects of bound CO.[35] The similarities among **1a**,**b** and **2a**−**d** suggest that ν(CO) is not a sensitive marker of such interactions in the present systems.

O_2 Binding. At ambient temperature, oxidation of the 5-coordinate species was instantaneous for all four hemes (**2a**−

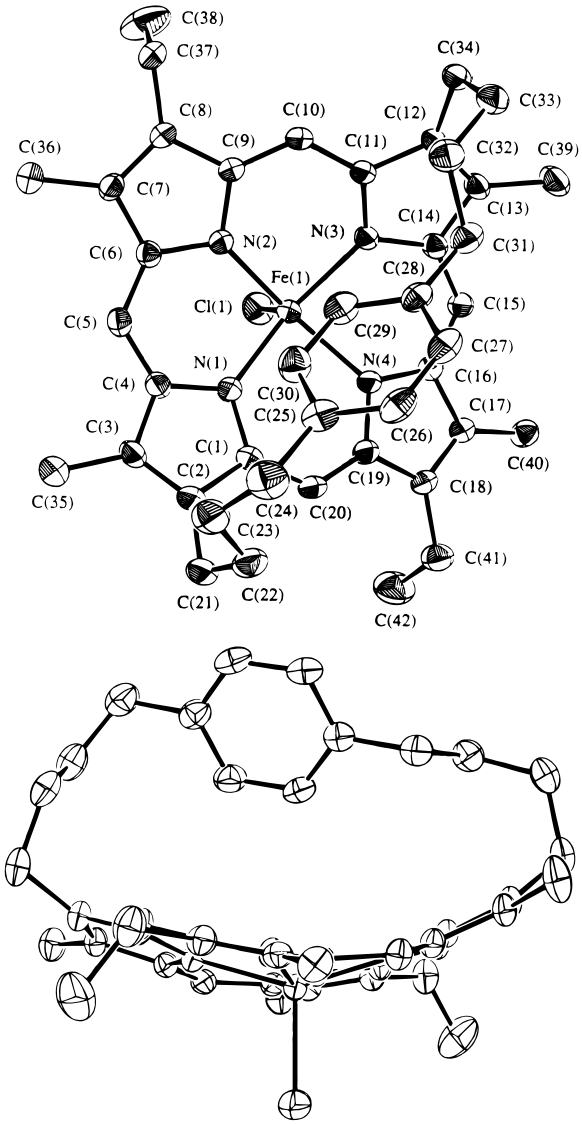

Figure 4. Face and edge views of **2a** as its ferric (Cl^-) complex.

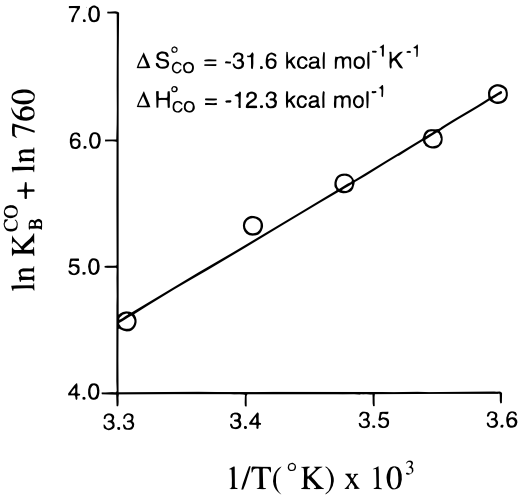

Figure 5. Van't Hoff plot for the carbonylation of **2a** in toluene.

d), and the UV/visible spectra showed that μ-oxo dimers had been formed. Therefore studies on O_2 binding were carried out at lower temperatures.

(35) Ray, G. B.; Li, X.-Y.; Ibers, J.; Sessler, J. L.; Spiro, T. G. *J. Am. Chem. Soc.* **1994**, *116*, 162−176.

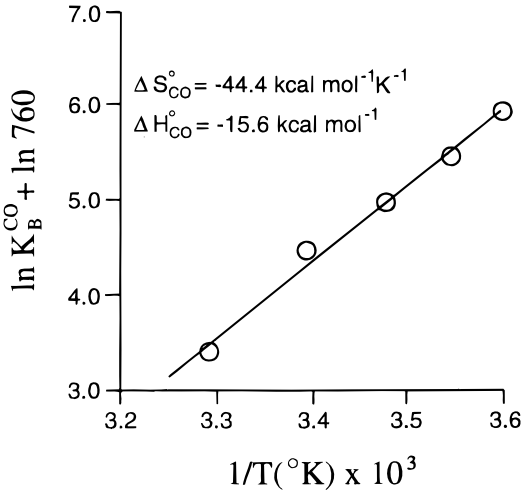

Figure 6. Van't Hoff plot for the carbonylation of **2c** in toluene.

Table 4. Thermodynamics Constants for CO Binding in Toluene[a]

heme	$\Delta H^{\circ CO}_B$, kcal mol^{-1}	$\Delta S^{\circ CO}_B$, cal mol^{-1} K^{-1}
Fe(durene-4/4)(DcIm)[b] (**1a**)	−9	−12
Fe(benzene-4/4)(DcIm) (**2a**)	−16	−44
Fe(amidobenzene-4/4)(DcIm) (**2c**)	−12	−32

[a] Standard state 1 atm. [b] Reference 28d.

Table 5. Infrared ν(CO) Values in Toluene

compd	ν(CO), cm^{-1}	K_B^{CO}, M^{-1}	compd	ν(CO), cm^{-1}	K_B^{CO}, M^{-1}
1a	1987[a]	2×10^6	**2c**	1980	2.8×10^4
1b	1985[a]	2×10^5	**2d**	1978	3.3×10^6
2a	1986	1.2×10^4	**3a**	1951[b]	4.0×10^8 [c]
2b	1982	1.6×10^4			

[a] 1,2-Dimethylimidazole as axial ligand.[28d] [b] DMSO. [c] Toluene−CH_2Cl_2 (9:1).[34]

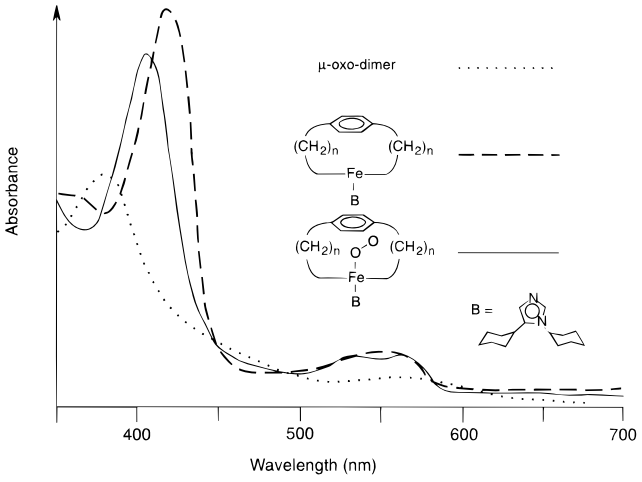

Figure 7. Optical spectra for the μ-oxo dimer and dioxygen complex of **2b** ($n = 5$).

Several temperatures were examined and −45 °C was found to be most suitable. Prolonged exposure to O_2 was avoided in order to minimize oxidation of the hemes; therefore, the spectral changes for only four O_2 concentrations were examined. A large excess of DcIm had to be maintained ([DcIm]:[heme] $\sim 10^5$) in all cases to effectively thwart irreversible oxidation to the μ-oxo dimer. Spectra for the μ-oxo dimer, the 5-coordinate complex, and the O_2 adduct for the Fe(5/5-benzene) system (**2b**) are shown in Figure 7. O_2 titration for all of the 5-coordinate hemes gave absorbance changes with clean isosbestic points

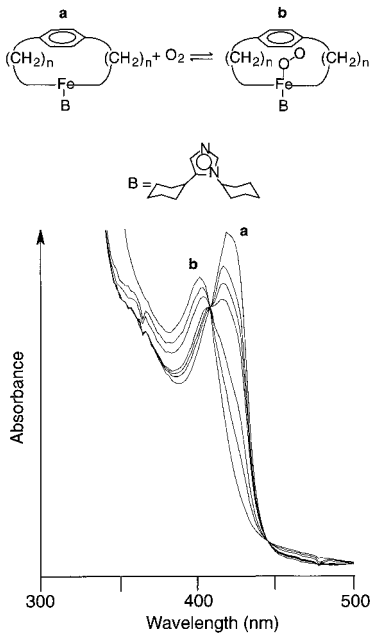

Figure 8. Isosbestic changes observed for the oxygenation of **2a** (n = 4) at −45 °C in toluene. P^{O_2} = 9.76, 30.95, 77.16, 163.69 Torr. Final P^{O_2} = 1 atm.

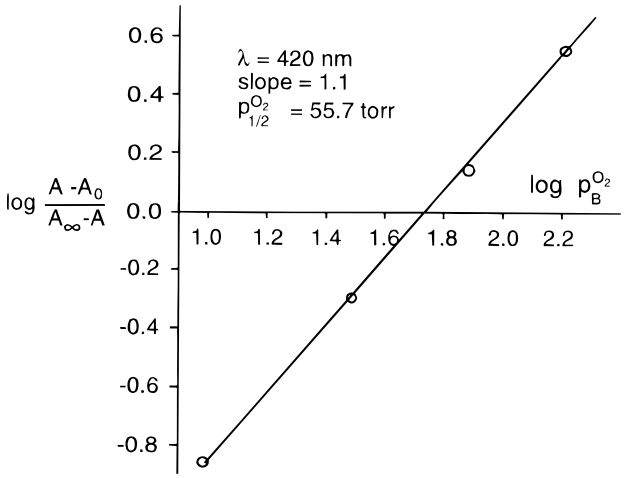

Figure 9. Hill plot for the oxygenation of **2a** at −45 °C in toluene.

Table 6. $P_{1/2}^{O_2}$ Values for Dioxygen Binding to the Capped Hemes in Toluene

heme	no.	$P_{1/2}^{O_2}$(20 °C), Torr	$P_{1/2}^{O_2}$(−45 °C), Torr
Fe(durene-4/4)(DcIm)[a]	**1a**	167	0.094[b]
Fe(durene-5/5)(DcIm)[a]	**1b**	∼64	
Fe(durene-7/7)(DcIm)[a]	**1c**	∼64	
Fe(benzene-4/4)(DcIm)	**2a**		55.7
Fe(benzene-5/5)(DcIm)	**2b**		22.7
Fe(amidobenzene-4/4)(DcIm)	**2c**		9.5
Fe(amidobenzene-5/5)(DcIm)	**2d**		2.8

[a] Reference 28d. [b] Extrapolated from thermodynamic data.

(Figure 8), indicating a clean conversion to the oxo species according to eq 2.

$$\mathrm{Fe(Por)(DcIm)} + \mathrm{O_2} \overset{K_B^{O_2}}{\rightleftharpoons} \mathrm{Fe(Por)(DcIm)(O_2)} \qquad (2)$$

Deoxygenation, by pumping after full formation of the O_2 complex, regenerated the 5-coordinate heme with negligible heme oxidation, confirming the reversibility of O_2 binding in these systems at −45 °C. The benzene- and amidobenzene-capped hemes were oxidized by dioxygen at room temperature; the flexible cap is presumed to swing to one side and allow the benzene moiety to become perpendicular to the porphyrin plane (Figure 4), thus allowing for μ-oxo dimerization. At lower temperatures (−45 °C), "dimerization" was slowed down and reversible dioxygen binding achieved.

An example of a Hill plot is shown in Figure 9, and the affinity constants for O_2 binding to our system together with those for the durene systems are recorded in Table 6. The data show strikingly high $P_{1/2}$ values for our system at low temperatures (−45 °C). However, within each pair of the benzene and amidobenzene hemes, a 6−8-fold increase in O_2 affinity is observed for the amide-substituted complexes (a free energy gain of ∼1 kcal/mol for the amidobenzene-4/4 heme (**2c**) and for the amidobenzene-5/5 heme (**2d**), relative to their corresponding non-amido hemes (**2a**,**b**)), which would be consistent with a possible hydrogen-bonding stabilization of the O_2 complex.

In the durene series the hydrophobic "cap" provides a relatively nonpolar distal environment so that (lack of) polarity effects experienced by the bound dioxygen should be identical for all three durene hemes. Any difference in O_2 affinities should therefore be caused by steric effects alone. Examination of the durene heme system reveals that at 20 °C the $K_B^{O_2}$ values of the Fe(durene-7/7) and Fe(durene-5/5)(DcIm) systems are identical and the difference of $K_B^{O_2}$ values between Fe(durene-5/5)(DcIm) and Fe(durene-4/4)(DcIm) is only 2-fold, indicating very small steric effects on O_2 binding in spite of the different cap sizes.

At −45 °C, the benzene− and amidobenzene−heme systems gave a very small (2−3-fold) increase in O_2 affinity for the 5/5-capped hemes relative to the 4/4-capped hemes. This is consistent with the trend found in the durene series. Perhaps the distortion (doming) of the 4/4-hemes accounts for this decreased $K_B^{O_2}$. Porphyrin skeletal doming of this type may be viewed as imparting "T-state" character to the 5-coordinate heme complex and hence a lower O_2 affinity.

Although the CO binding affinities of the corresponding benzene− and amidobenzene−heme complexes are different (∼2-fold increase for the amide-substituted analogues), the influence of a similar steric effect can be excluded as the only source for the higher O_2 affinity enhancement for the amide analogues when compared with the non-amide hemes. The O_2 affinity enhancement of the analogous amide is 6−8-fold, too large to be accounted for by a steric effect alone. Therefore, either the polarity of the distal cage or a direct interaction of the amide proton with bound dioxygen contributes to this increased O_2 affinity for the amidobenzene hemes.

Within each pair of the benzene and amidobenzene hemes, the only difference in structure is the amide functionality. In the free-base amide-substituted porphyrin, the N−H of the amide group is shifted upfield in the NMR spectrum compared to normal aromatic amide protons,[29a] indicating that this proton is situated near the center of the porphyrin plane, suggesting that a direct interaction of the amide N−H with O_2 (H-bonding) is possible.

Compared to the case of the basket-handle models of Momenteau et al. and Chang and Kondylis's porphyrin naphthoic acid series[22c] the O_2-adduct gain in stability of the amidobenzene hemes due to an amide group is not very large with the present systems. The basket-handle model has a 10-fold increased O_2 affinity and the porphyrin naphthoic acid series has an even larger O_2 affinity. The smaller O_2 affinity increase of our system can be explained in terms of hydrogen-bonding strength. Even though the H and O atoms might achieve an

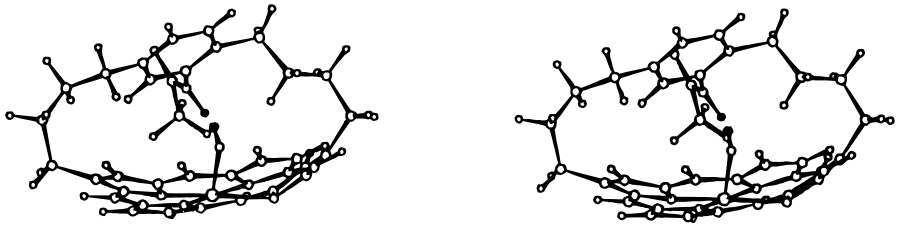

Figure 10. Stereoview of a conformation of oxygenated **2c** showing N−H···O hydrogen-bonding (structure minimized using InsightII (Biosym, San Diego)).

approximate orientation for hydrogen-bonding, the benzene cap is able to rotate and swing to one side of the heme and N−H···O need not remain linear. Indeed molecular modeling shows that a number of conformations are possible where hydrogen-bonding can take place (Figure 10).

Conclusion

Introduction of an amide functionality to the distal cage of hemes **2c**,**d** increases their O_2 affinity due to the interaction between the polar amide function and the bound dioxygen. Therefore a comparison between the benzene hemes (**2a**,**b**) and amidobenzene hemes (**2c**,**d**) gives quantitative support for the hypothesis that hydrogen-bonding plays an important role in differential binding of CO and O_2 by hemoglobin and myglobin.

Acknowledgment. This work was supported by the Natural Sciences and Engineering Research Council of Canada. We thank Professor B. R. James for his insightful comments.

Supporting Information Available: A description of the X-ray experimental procedures, tables of crystal data, experimental details, positional parameters, thermal parameters, bond distances, bond angles, torsional angles, intermolecular contacts, and least-squares planes, and additional structural diagrams for **2a** (41 pages). Ordering information is given on any current masthead page.

IC9600745